ISSN 1063-7729, Astronomy Reports, 2006, Vol. 50, No. 11, pp. 926–935. © Pleiades Publishing, Inc., 2006.
Original Russian Text © I.M. Livshits, V.N. Obridko, 2006, published in Astronomicheskiĭ Zhurnal, 2006, Vol. 83, No. 11, pp. 1031–1041.

Variations of the Dipole Magnetic Moment of the Sun during the Solar Activity Cycle

I. M. Livshits and V. N. Obridko

Pushkov Institute of Terrestrial Magnetism, the Ionosphere, and Radiowave Propagation, Troitsk, Russia

Received February 28, 2006; in final form, March 13, 2006

Abstract—Observations of the large-scale solar magnetic field (synoptic maps) and measurements of the magnetic field of the Sun as a star (the total magnetic field) are used to determine the dipole magnetic moment and direction of the dipole field for three successive solar cycles. Both the magnetic moment and its vertical and horizontal components vary regularly during the cycle, but never disappear completely. A wavelet analysis of the total magnetic field shows that the amplitude of the 27-day variations of this field is very closely related to the magnetic moment of the horizontal dipole. The reversal of the global dipole field corresponds to a change in the inclination of its axis and occurs in a series of steps lasting one to two years rather than continuously. Before the onset of the reversal, the dipole axis precesses relative to the solar rotational axis, then shifts in a meridianal plane, reaching very low latitudes, where a substantial shift in longitude then begins. These results are discussed in connection with helioseismological data indicating the existence of oscillations with a period of about 1.3 yr and properties of dynamo processes for the case of an inclined rotator.

PACS numbers : 96.60.Hv
DOI: 10.1134/S1063772906110060

1. INTRODUCTION

The most important phenomena of the solar activity are associated with the evolution of local magnetic fields that leads to the formation of sunspots and active regions—structures with sizes of several arcminutes. The large-scale fields on the Sun are not visible in observations with high spatial resolution, but can be clearly distinguished in the Standford synoptic maps, with a spatial resolution of $3' \times 3'$. Conventionally, we distinguish local (sizes of several arcminutes) and large-scale (sizes from several arcminutes to $10'$–$20'$, i.e., ~ 0.2–$1\ R_\odot$) fields in solar magnetic maps. The large-scale fields include two latitude regions occupied by fields with opposite directions, and a set of quasi-unipolar structures at middle and low latitudes with sizes from several arcminutes to $10'$–$20'$. These quasi-unipolar magnetic regions, which sometimes form from the remnants of large active regions, exist from half a year to one or two years. The largest-scale field is associated with the dipole component of the solar magnetic field, i.e., the global solar dipole.

It is known, primarily from eclipse observations, that, in the case of very low activity, the coronal magnetic field represents to some extent a global dipolar field whose axis nearly coincides with the solar rotational axis. We are speaking here of coronal layers in which the speed of the solar wind is still low, below the "surface source" of the solar wind. In this phase of the activity cycle, perturbations of the dipolar structure by local fields are weak. This magnetic configuration remains stable for several years.

At lower latitudes, the dipolar configuration of the global field facilitates the development of high coronal loops, each of which joins regions of oppositely directly magnetic fields on opposite sides of the equator. This leads to the formation of a large-scale coronal structure at the cycle minimum displaying a belt of streamers near the equator at all longitudes and two systems of polar plumes. As a result of the solar wind carrying away the global magnetic fields into interplanetary space, a heliospheric current sheet develops, which divides regions with oppositely directed magnetic fluxes. This neutral current sheet is planar in periods of low activity.

With growth in the activity, the influence of active regions increases, and the polarity dividing line for the large-scale magnetic fields near the equator becomes corrugated. In addition, the role of the quadrupolar component and higher harmonics of the large-scale magnetic fields becomes more important in such periods.

Direct observations of large-scale fields are available for the last few cycles. In addition, starting from 1968, the Crimean Astrophysical Observatory (CrAO), and then other observatories, began to carry

out observations of the magnetic field of the Sun as a star (the total magnetic field, TMF). The TMF signal is proportional to the solar magnetic-field intensity integrated over the central part of the disk. The main contribution is made by large-scale fields. These two sets of observations can be used to study the characteristics of the large-scale fields over the past few cycles.

Appreciable progress in the development of the dynamo theory and helioseismological studies has been made in recent years. Unfortunately, studies in these areas have not fully taken into account the available observations of solar magnetic fields. In particular, when considering the generation of magnetic field inside the Sun, it is usual to assume that the solar dipole moment vanishes completely at the onset of the polarity reversal near the maximum of the solar cycle, then appears again with the opposite sign [1]. This provides additional motivation to return to the question of the contribution of the dipolar component to the observed solar magnetic field.

We first give below a brief description of the available observations of the large-scale fields and methods used to distinguish the dipolar component. We then consider the behavior of the field of the Sun as a star and of the dipolar components calculated based on synoptic maps for the last three cycles. We compare the results of a wavelet analysis of a time series of TMF values and the calculated characteristics of the dipolar field, in order to characterize any regular behavior observed. In conclusion, we summarize our results and briefly discuss their importance for the dynamo theory, helioseismology, and the physics of interplanetary magnetic fields.

2. INITIAL OBSERVATIONAL MATERIAL AND ANALYSIS METHODS USED

We used magnetic-field measurements obtained at the Stanford University Solar Observatory (now the Wilcox Solar Observatory; http://quake.stanford.edu/wso/wso.html). The corresponding values of the longitudinal component of the photospheric magnetic field were transformed into synoptic maps for each Carrington revolution [2, 3].

We used an expansion of the observed magnetic field in spherical functions (Legendre polynomials) in our subsequent analysis. Further, we calculated the magnetic dipole moment μ and the latitude θ of the north (N) pole of the magnetic dipole for data obtained in Carrington revolutions 1642–2027 (1976.44–2005.2), as well as the magnetic moments of the "vertical" μ_{vert} and "horizontal" μ_{horiz} dipole components, using the formulas

$$\mu_{full} = \sqrt{g_{10}^2 + g_{11}^2 + h_{11}^2},$$

$$\mu_{vert} = |g_{10}|,$$

$$\mu_{horiz} = \sqrt{g_{11}^2 + h_{11}^2},$$

$$\sin\theta = g_{10}/\mu,$$

where g_{10}, g_{11}, and h_{11} are the coefficients for the expansion of the observed magnetic field in Legendre polynomials.

We carried out the calculations in the classical way, assuming potential behavior from the photosphere to the source surface at a height of 2.5 $R_\odot$ from the solar center and introduced a polar correction to take into account the uncertainty of magnetic-field measurements near the poles [4]. Note, however, that our results do not depend on these assumptions.

In addition, our analysis is based on a series of daily values of the solar TMF. In principle, these data can also be used to study variations in the dipole component of the global magnetic dipole. By means of illustration, Fig. 1 presents values of the solar TMF for 1984 and 1991 derived from a series of values obtained at various observations and reduced to a single series [5]. Figure 1 clearly displays the presence of variations with a period of about 27 days. The amplitude of these variations is large in some periods near activity maximum and decreases to very small values in the transition to activity minimum. The difference in the maximum TMF values in 1984 and 1991 in Fig. 1 is in agreement with detailed studies carried out at the CrAO [6]. The exact value of the dominating period was also elucidated during earlier investigations at the CrAO [6, 7].

Figure 1 also compares the TMF values for 1991 measured directly and calculated by averaging synoptic maps. We can see from these data that the TMF signal does indeed correspond to the mean field for the central part of the solar disk. Note that the activity was fairly high in 1991, including the presence and development on the disk of large groups of spots (indicating strong local fields). In quieter periods, the agreement between the TMF values and the mean values calculated from synoptic maps is much better than in the lower panel in Fig. 1.

Figure 1 provides some evidence that variations of the TMF are related to the behavior of the global dipole. However, we continued this study in order to investigate which characteristics (components of the magnetic moment, their magnitude and direction) determine the variations of the TMF at various phases of the solar cycle. Our analysis of TMF data for 1975 to 1996 below is also based on observations carried out at the Stanford Observatory. We analyzed this time series using a wavelet-analysis program based on the gapped wavelength algorithm [8], which pays special attention to eliminating the effect of gaps in the data. Test computations showed the high effectiveness of

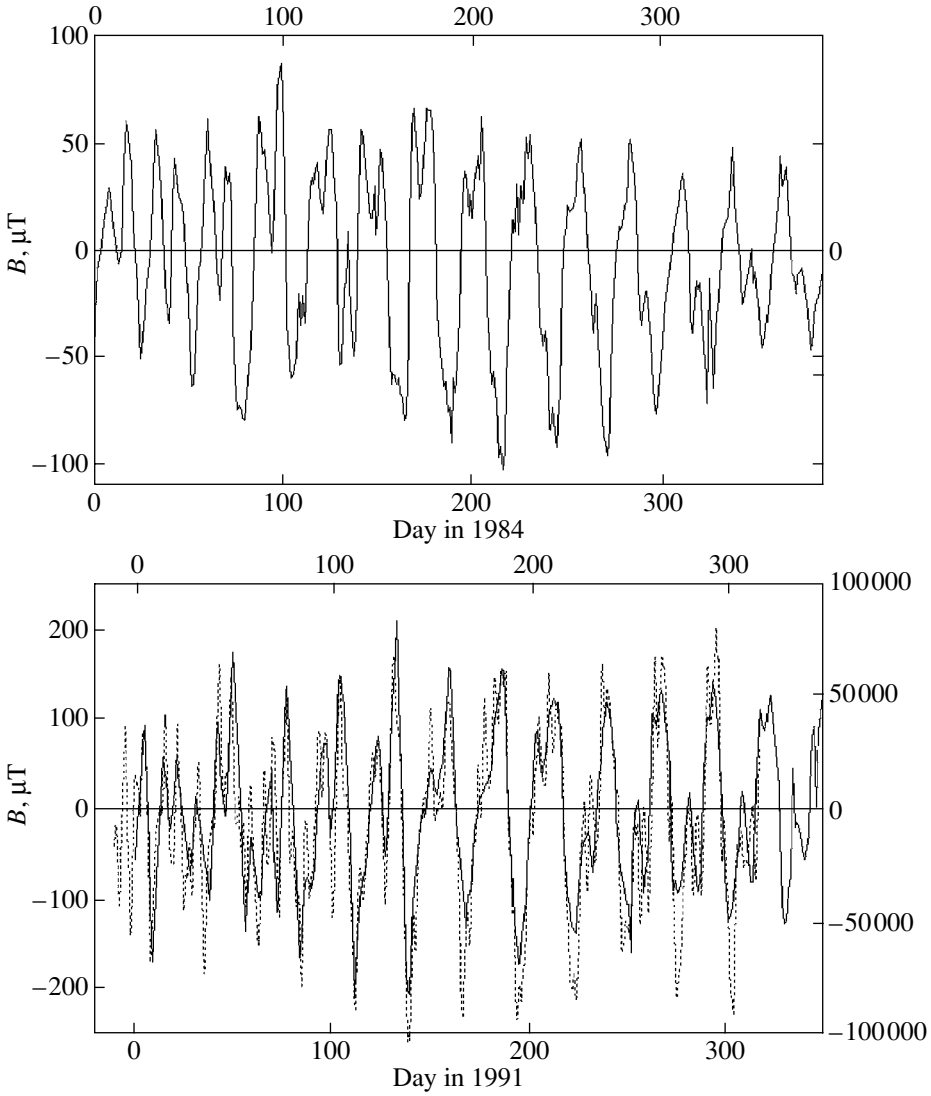

Fig. 1. Magnetic field of the Sun as a star in microtesla (100 μT $\equiv$ 0.01 G) in 1984 and 1991 based on the Stanford observations (solid curves). The dotted curve represents values calculated using photospheric data for the solar TMF in arbitrary units (right scale).

the program when applied to data series with large gaps. In the case of this series of TMF values, when gaps occupy about 15% of the entire observing interval, this proved to be better than filling the gaps with data from other observatories. As usual, the main difficulty in reducing various data to a single series is eliminating differences in the calibrations used for different instruments.

3. CYCLICAL VARIATIONS IN THE GLOBAL DIPOLAR FIELD AND ITS COMPONENTS

The results of our calculations of the magnetic moment of the dipolar component and its individual components are presented in Figs. 2 and 3. We can see that the total absolute value μ_{full} is nearly always in the range 20–40 $\mu\mathrm{T}/R_\odot^3$; i.e., it varied by no more than a factor of 2–2.5 during the course of two and a half cycles.

We emphasize that the dipole magnetic moment never vanishes completely. Strictly speaking, this assertion is based here on data with a time resolution of only 13–14 days, but very rapid variations of the magnetic fields on scales comparable with the solar radius are not possible. Moreover, the disappearance of the global magnetic field would lead to appreciable variations in the structure of the coronal at heights of more than 1.2–1.5 $R_\odot$. An examination of the daily SOHO LASCO-2 observations indicates that no such anomalous cases are observed.

Comparison of the time variations of the total dipole moment with the phase of the solar cycle

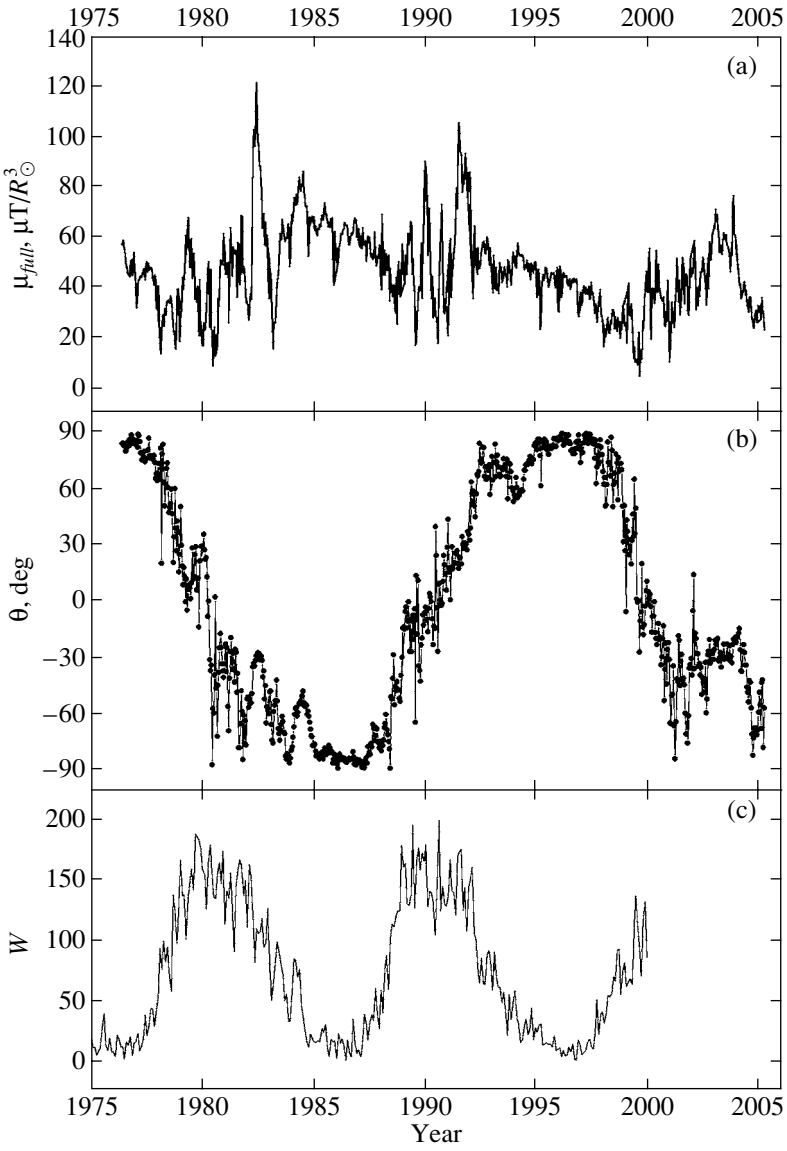

Fig. 2. (a) Total dipolar magnetic moment μ_{full}. (b) Inclination angle θ for the magnetic-dipole axis measured from the solar equatorial plane (its latitude); the time resolution is half of a Carrington revolution. (c) Mean monthly Wolf numbers.

(Fig. 2a) and the Wolf number (Fig. 2c) indicates that the minimum magnetic moment does not always coincide with the characteristic points of the cycle. This minimum value is usually achieved in the growth or decay phase of the solar cycle. Cyclical variations in the total magnetic moment and both its components can be seen (Figs. 2 and 3) and are most clearly distinguished in the variations of the angle θ.

The fact that the magnetic dipole is strictly vertical at the cycle minimum is reflected in Fig. 2 by the fact that the horizontal dipole vanishes at this epoch, and the latitude of the dipole axis becomes close to 90°. With approach toward the cycle maximum, the total magnetic moment varies strongly at some times, but never vanishes.

In the decay phase of the cycle, a state in which the vertical and horizontal magnetic moment components are comparable is established for one to two years. This situation is referred to in astrophysics as an inclined rotator. We can see that this situation is realized in years of high activity, and is manifest most clearly in the second maximum of the coronal activity and the onset of the decay phase in 1982 and 1984, then ten years later in 1992 and 1994. The pattern in the activity cycle that has just passed is not so clear.

The tendencies discussed above also appear in Fig. 3, where the total dipole magnetic moment is compared with its vertical and horizontal components. The vertical component smoothed over several revolutions varies smoothly and clearly demonstrates

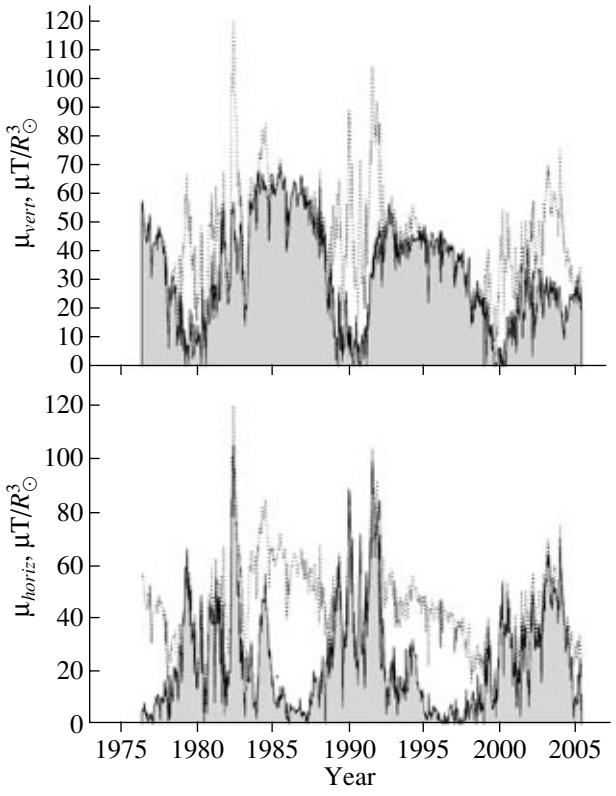

Fig. 3. Behavior of the (a) vertical μ_{vert} and (b) horizontal μ_{horiz} components of the global magnetic dipole with time. The area above the curves is shown in gray. The thin curve in both graphs shows the behavior of the total magnetic moment (in the same units).

ten-year cyclical variations. The horizontal component appears in each cycle at periods of high activity, close to the epochs of polarity reversals. It sometimes takes on large values compared to the vertical component, and is characterized by a fairly large scatter. It is possible that this is partly associated with variations with a period of one to two years (see discussion below). Comparing the components with the total dipole moment again illustrates the fact that an essentially vertical dipole is realized at the cycle minima, and an essentially horizontal dipole near the cycle maxima.

Figure 3 also shows the presence of strong variations in the behavior of both components in the 21st and 22nd cycles compared to their variations in the 23rd cycle. The main difference of the cycle that has just passed is that the activity at the maximum was modest, but continued longer than is usual—for about five years. Note that, since the ratio of the horizontal and vertical components is $\tan\theta = \mu_{horiz}/\mu_{vert}$, some regularities can also be traced in Fig. 2.

In concluding this section, we reiterate that cyclical variations can be clearly traced in the dipolar magnetic moment and its individual components.

4. ROTATIONAL VARIATIONS IN THE TMF SIGNAL

Let us now turn to information about the dipole component that can be derived from the variations of the TMF. We can already see from these data that the amplitude of the 27-day variations is large at activity maximum and decreases to very low values in the transition to activity minimum. This was studied earlier by Haneychuk [6] for each year in the interval 1968–1996. Cases of high amplitudes are presented in Fig. 1 for 1984 and 1991.

However, it is of interest to compare the behavior of these oscillations for the characteristic life times of the solar dipole. We began such an analysis earlier in [9] for the cases of a horizontal and oblique dipole. The former situation is manifest most clearly in 1991, when a streamer belt was observed near the solar pole at some times, with the spherical corona typical of an epoch of maximum, again, appearing a fourth of a solar revolution later. In [9], we divided each of the intervals in which modulation of the TMF signal (the master data series of [5]) was clearly visible into 27-day intervals, with the beginning of the oscillation in the center of the interval, coincident with the onset of the day for the corresponding Carrington revolution (CR). We found that the 27-day variations of the TMF were most clearly manifest in 1984, in CR 1748–1753. This situation is not very rare, and one or more intervals with durations of about half a year and with a similar set of phase dependences can be identified in the decay phase of each cycle. The amplitude of these variations was somewhat higher in the second half of 1991 than in 1984, and their shape was more complex, reflecting the influence of the quadrupole component of the magnetic field.

Note that, as in August 1972, the disruption of the regularity of the 27-day variations in June 1991 is, of course, related to the appearance of more activity complexes and the intensification of processes at the active longitude.

Wavelet analyses present considerable opportunities for studying periodic variations of signals whose amplitude varies within time intervals appreciably exceeding the period for the main mode. The distribution of the amplitudes of the wavelet transform of the time series of Stanford TMF values is shown in Fig. 4. We present here the results for our computations with the best resolution along the x direction (with the value of the coefficient k in the expression for the wavelet transform [8] equal to four). Each ten years, we can see well defined peaks of this distribution with $A \approx 100$ for periods close to 27 days. Of course, the years with high amplitudes for the rotational modulation of the TMF (1983, 1990–1991) agree with conclusions drawn earlier [6, Fig. 5]. The second harmonic of these variations is expressed quite clearly. In the data for

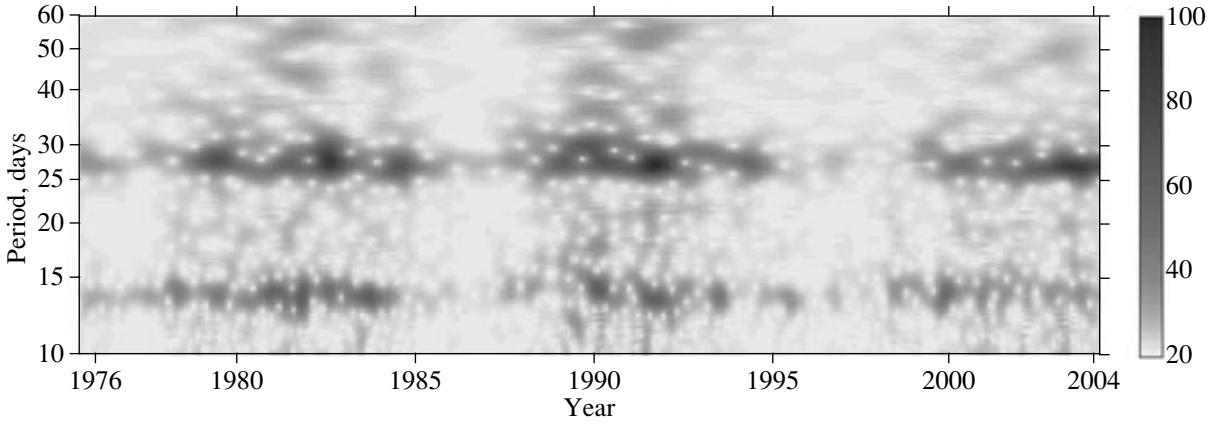

Fig. 4. Distribution of the amplitudes of the wavelet transform of the time series for the solar TMF values in period–time coordinates. The scale for the amplitudes A per unit frequency interval is given to the right.

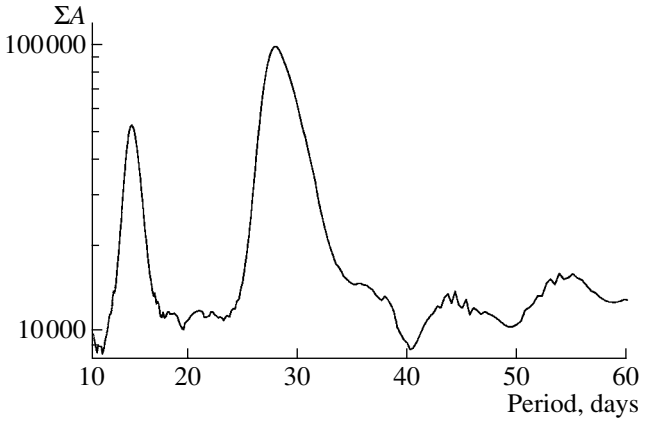

Fig. 5. Sum of the amplitudes of the wavelet transform shown in Fig. 4 as a function of period (analogous to the Fourier power spectrum for the entire dataset of solar TMF values). In the wavelet analysis used, the time resolution was maximum, leading to some smoothing of the presented frequency spectrum.

both the main mode and the second harmonic, we can distinguish some one-to-two-year time intervals when TMF variations with a period of about 30 days appear.

The presence of variations with periods appreciably greater than 27 days is also manifest in the sum of the amplitudes for the wavelet analysis in a given frequency interval—analogous to the Fourier spectrum. The corresponding dependence for the entire studied time interval as a function of the period is presented in Fig. 5. We present in this figure results for our computations with $k = 4$, whose frequency resolution is not very high. We can see a difference in the left and right wings of the main maximum. A component with a period of 30 days is manifest more distinctly in the computations with $k = 2$. This frequency structure in the period interval 26–30 days (13–15 days at the second harmonic) reflects the differential rotation of the magnetic fields on the Sun, and further in interplanetary space.

The use of a wavelet transform enables us to elucidate the reason for the appearance of TMF variations with a period of 27 days. Figure 6 compares the variations in the amplitude of the wavelet transform for the 27-day period with the variations in the horizontal component of the magnetic dipole moment. The section of the distribution of A presented in Fig. 4 for a period very close to 27 days is characterized by maxima that are nearly identical to the maxima of the horizontal component of the magnetic dipole moment. In addition to the tendency for rigid-body rotation of the sources of magnetic fields on the largest scales, we apparently see here, as well, a manifestation of the polarity-reversal process (see below).

We emphasize that large values of the horizontal magnetic moment are observed in periods of high activity, when spots and the corresponding local fields are present on the disk in great numbers. Nevertheless, the field of the Sun as a star is primarily associated precisely with the position of the dipole axis.

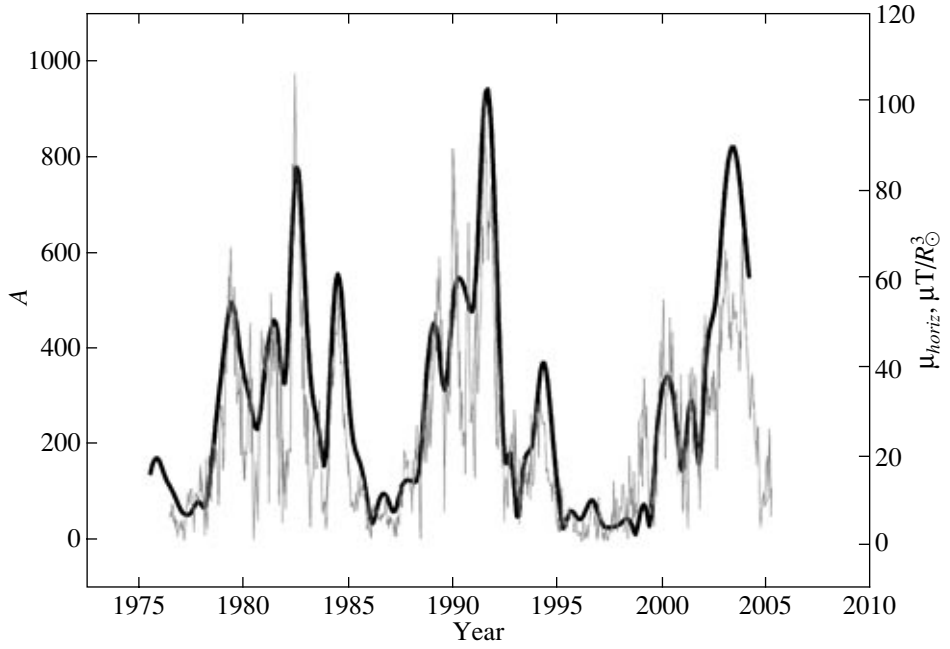

Fig. 6. Time run of the amplitudes of the wavelet transform shown in Fig. 3 for a period of 27.0 days (bold curve). Here, the absolute values A correspond to several unit frequency intervals. The thin curve shows the values for the horizontal component of the dipole (scale presented to the right).

In other words, an oblique rotator arises on the Sun not when the dipole moment vanishes but instead when it takes on large, or even its largest, values. The polarity-reversal process is associated precisely with a rotation of the dipole-moment vector.

5. COORDINATES OF THE NORTH POLE OF THE DIPOLE AND ITS VARIATIONS DURING THE CYCLE

Let us now consider the cyclical variations of the position of the north pole of the total dipole on the Sun in both latitude and longitude. By definition, the latitude of the pole of the vertical dipole is $\pm 90°$ and its longitude is not defined; the latitude of the pole of the horizontal dipole, which is parallel to the equatorial plane, is always equal to zero, while its longitude is a distinguishing characteristic. The position of the north pole of the total dipole on a sphere depends on the longitude of the horizontal dipole and the ratio of the moduli of the vertical and horizontal components.

Figure 7 gives for each Carrington revolution in cycles 21–23 the position of the northern magnetic pole on the solar surface in the coordinate system (θ, λ), where these two coordinates represent the latitude and longitude of a point on the solar surface, respectively. Note that, in this representation, the polar latitudes are more extended than the equatorial regions. The center of this coordinate system is the geographic pole of the corresponding hemisphere of the Sun. The upper diagrams refer to the north pole and the lower diagrams to the south pole.

At the end of cycle 20 and the beginning of cycle 21, the N field was located at the northern polar cap. Accordingly, the upper diagram of the figure for the 21st cycle shows data for CR 1643–1665 (the polar field in 1976.5–1978.2) and then for the polarity reversal during CR 1666–1692 in 1978.2–1980.2. In the lower diagram for the 21st cycle, the data for the polarity reversal refer to CR 1692–1697 (1980.25–1980.66) and for the "polar field" to CR 1697–1737.

The N field occults the southern polar cap at the beginning of the 22nd cycle. The corresponding points, which are for CR 1737–1801 (1983.6–1988.3) and describe the position of the N pole of the dipole, are located in the lower diagram (squares). Further, data for CR 1801–1828 (1988.3–1990.3) in the lower diagram and for CR 1829–1857 (1990.4–1992.5) in the upper diagram are presented for the period of the polarity reversal. The polar field at the end of the even cycle 22 (stars) is presented for CR 1857–1900 (1992–1995.7).

The pattern for the odd cycle 21 is repeated at the beginning of the 23rd cycle. Data at the beginning of this cycle are presented for CR 1901–1941 (1995.8–1998.8). Further, during the polarity reversal, the N pole of the dipole is first located in the northern hemisphere during CR 1941–1963, then in the southern hemisphere during CR 1959–2018. Finally, the polar

field at the end of the 23rd cycle is represented by data for CR 2018–2036 (2004.6–2005.9).

We can see from Fig. 7 that, during the cycle minimum, the dipole axis describes a fairly regular shift relative to the rotational axis, reminiscent of precession. Over the period of the minimum, the dipole moves around the rotational axis, performing one or two turns. This quasi-precessional motion continues for one to three years, and it is precisely during this time that the oblique rotator is realized. This is followed by a fairly sharp jump into the equatorial region, taking 0.7–1.2 years. Further, the dipole continues a smooth motion in longitude in the near-equatorial region over 1.5–3 years. This is followed by a new jump, and the precessional motion continues about the opposite pole.

Note that the different rates of variation in latitude are also manifest in Fig. 2, as variations in the inclination angle $d\theta/dt$. The latitude of the dipole axis varies more rapidly at the beginning and end of the polarity-reversal process, while the variations at low latitudes occur more slowly. For example, in cycle 22, the active latitude changed rapidly up until the beginning of 1990, then again in 1992 (Fig. 2), with the variations in 1990–1991 being much slower; corresponding behavior can be followed in the decay phase of this cycle near 2000.

The quasi-precessional motion makes it clear that variations with time scales near 1.5 to 2.5 years are not manifest only at epochs of high activity but also remain appreciable when the Sun is virtually quiescent.

The variations in the position of the dipole axis in the 23rd cycle compared to those in cycles 21 and 22 can also be traced in Fig. 7. For the northern hemisphere, these consist of quasi-precession with a somewhat lower amplitude and an unusual drift in longitude and latitude in 1998. This last cycle is known to be unusual in many ways; in particular, its maximum was very poorly expressed, and the activity decay proceeded very slowly. Note also that, for the three activity cycles considered, the motion of the dipole axis was more regular in the northern hemisphere than in the southern (Fig. 7). This asymmetry is probably due to secular variations of the solar activity.

6. VARIATIONS IN THE CHARACTERISTICS OF THE MAGNETIC-DIPOLE VECTOR WITH A PERIOD OF 1–2 YEARS

We noted above that the characteristics of both the total dipole-moment vector and its components vary with the period of the cycle. However, in addition to this quasi-eleven-year main oscillation mode, there appear to be shorter-period oscillations present in the data. Figure 8 shows separate Fourier spectra for the vertical and horizontal dipoles and shows the following:

1. The quasi-eleven-year cycle appears identically in the oscillations of the horizontal and vertical magnetic-dipole components. The full agreement in both period and amplitude indicates that these two sets of oscillations represent the same physical phenomenon, and there is no physical reason to make this separation into two types of oscillations from the point of view of the main solar-activity cycle. We are not dealing here with cyclical variations in the latitude of the axis of an oblique rotator.

2. The situation with regard to oscillations with periods of 1.3–2.5 years is completely different. These oscillations are present only in the data for the horizontal magnetic-dipole and are completely absent from the data for the vertical dipole. Their existence leads to the oscillations in the inclination of the total dipole noted by Gulyaev [10]. The coincidence with the helioseismological period of 1.3 years [11] suggests that these oscillations are related to the generation of magnetic field in the convective zone in the region of the tachocline. It is curious that the 1.3-year helioseismological oscillations, likewise, gradually disappear in the transition to higher latitudes, i.e., in the region where the vertical dipole is predominant.

7. CONCLUSIONS AND DISCUSSION

Thus, our analysis leads to a certain picture for the variations in the characteristics of the global dipole of the Sun during the course of the solar cycle. The vertical and horizontal dipole components clearly display cyclical variations that are more weakly expressed in the modulus of the total dipole vector. This is associated with a phase shift in the variations of these two components by approximately five years (half the cycle duration). The amplitude variations of the two components are very different. The vertical component varies more smoothly, reaching its maximum values at the cycle minimum. The horizontal component determines the maximum value of the total dipole field in periods of high activity. It is more variable and essentially determines the orientation of the total dipole-moment vector during the polarity-reversal process. The value of μ_{horiz} varies on time scales of one to two years. The global-dipole vector seems to precess in an irregular fashion about the rotational axis, then rotates essentially in a meridional plane during the polarity-reversal process; i.e., it moves along the same heliolongitude in each hemisphere.

Our results should be taken into account when analyzing certain problems in dynamo theory, helioseismology, and the physics of the interplanetary

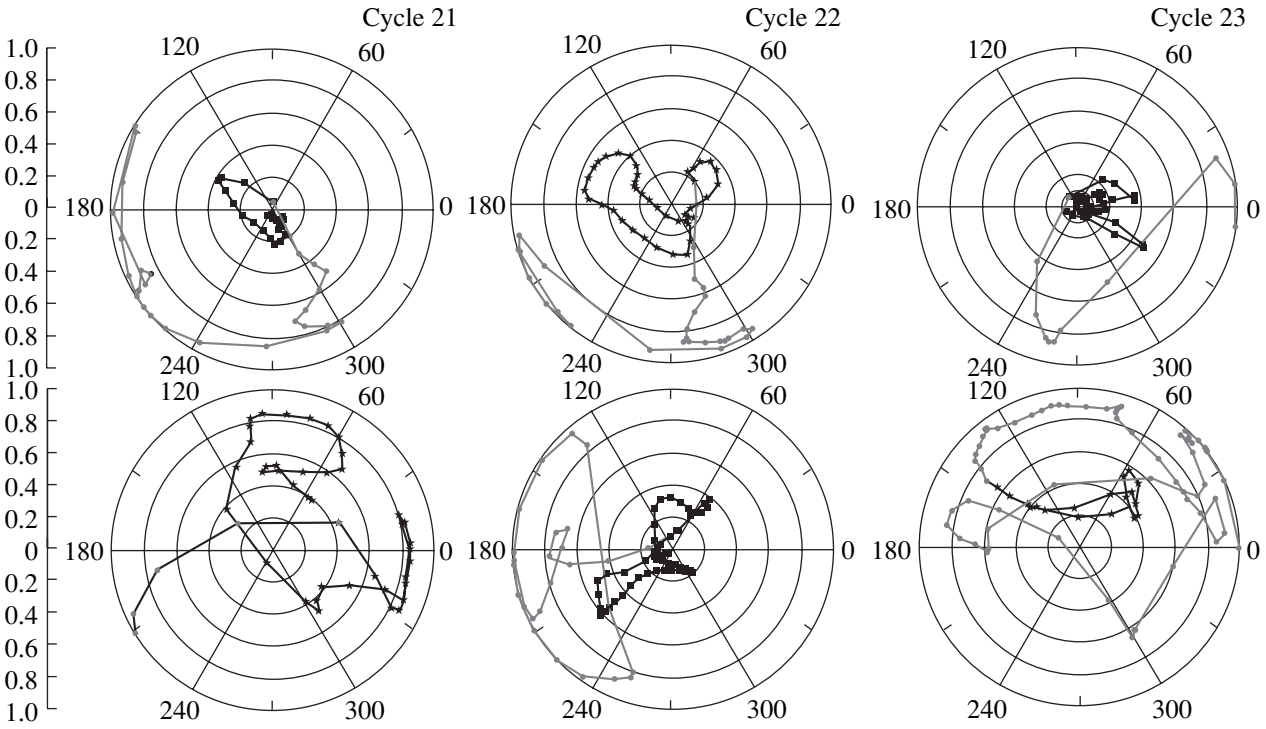

Fig. 7. Position of the N pole of the magnetic dipole for three solar cycles. The upper diagrams correspond to the northern hemisphere of the Sun, and the lower diagrams to the southern hemisphere. The circles represent contours of the $\cos\theta$ values presented on the vertical scales. The values of λ are in degrees. Data for the onset of each cycle are shown by squares, and those at the end of each cycle by stars (see text for more detail).

magnetic field. We note here that, in the case of a finite, nonzero, value for the magnetic-dipole moment of the Sun or another star during the polarity reversal, the generation and amplification of magnetic field will progress otherwise than has been assumed earlier. This should have the strongest impact on the dynamo problem when the dipole moment and rotational axis are not coincident. In other words, the theory for the generation of magnetic field in the case of an inclined rotator must assume that the dipole axis rotates during polarity reversal, rather than vanishing.

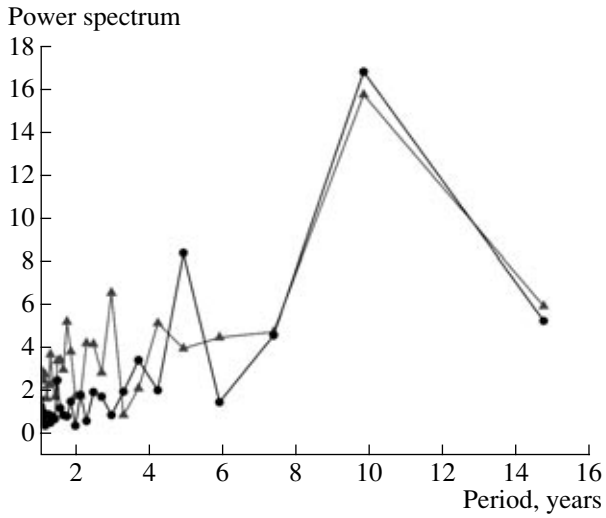

Fig. 8. Fourier power spectrum for the entire dataset for $B_\odot$. The circles correspond to the vertical component and the triangles to the horizontal component.

Moreover, there is reason to believe that the quasi-precessional motion we have discovered corresponds to real precession of the global dipole; i.e., this motion does not arise due to the influence of the development of large activity complexes—powerful local magnetic fields—on the disk. In this case, the generation and amplification of fields, which has been considered in periods of minimum activity assuming a purely poloidal field, must now take into account the presence of a weak toroidal ϕ component of the field. This could lead to a transformation of poloidal into toroidal field during the course of the cycle.

Another interesting result of this work is the detection of variations in the characteristics of the dipole field with a period of one to two years. These variations, which are best expressed in periods of high activity, very likely reflect variations in the orientation of the global dipole. It is of interest to study the relationship between this effect and the 1.3-year oscillations revealed by helioseismological data. Further, it is of

interest to compare our results with the helioseismology results for different phases of the cycle (see the review [12]), in particular, the torsional oscillations.

The standard model for the interplanetary magnetic field is based on the propagation of the large-scale magnetic fields of the Sun in the heliosphere. Its main feature is the appearance in interplanetary space of a corrugated current sheet and the formation of two latitude zones, in one of which the influence of this current sheet is strong, and in the other of which the force lines of the interplanetary magnetic field are close to radial and extend to large distances in the heliosphere. For periods of modest activity, this picture has been confirmed by observations with several spacecraft (primarily Ulysses). The question raised by our results is whether the conditions in the heliosphere vary strongly in the case of an oblique, or even horizontal, orientation for the global solar dipole during periods of high activity.

We note, as well, that the solar rotational axis and magnetic-dipole axis nearly coincide at activity minimum and that an observer on Earth is located in a plane perpendicular to the rotational axis. Therefore, the inclined rotator will be realized for an observer on Earth only during a comparatively brief time interval near the cycle maximum. On other stars, the magnetic-dipole axis could be inclined relative to the rotational axis, with the latter axis inclined to the line of sight by some angle. Therefore, observation of inclined-rotator situations could be the rule rather than the exception for observations of active late-type stars.

ACKNOWLEDGMENTS

The authors thanks D.D. Sokolov and M.A. Livshits for stimulating discussions of this work, and also V.V. Bruevich for help in carrying out the wavelet analysis. This work was supported by the Russian Foundation for Basic Research (project codes 05-02-16090 and 04-02-16068).

REFERENCES

1. S. V. Berdugina, D. Moss , D. D. Sokoloff, and I. G. Usoskin, Astron. Astrophys. **445**, 703 (2006).
2. J. T. Hoeksema and P. H. Scherrer, *The Solar Magnetic Field—1976 through 1985*, WDCA Report UAG-94 (NGDC, Boulder, 1986).
3. J. T. Hoeksema, *Solar Magnetic Fields—1985 through 1990*, Report CSSA-ASTRO-91-01 (1991).
4. V. N. Obridko and B. D. Shelting, Sol. Phys. **184**, 187 (1999).
5. I. V. Anan'ev and V. N. Obridko, Astron. Zh. **76**, 942 (1999) [Astron. Rep. **43**, 831 (1999)].
6. V. I. Haneychuk, Astron. Zh. **76**, 385 (1999) [Astron. Rep. **43**, 330 (1999)].
7. V. A. Kotov, V. I. Haneychuk, and T. T. Tsap, Astron. Zh. **76**, 218 (1999) [Astron. Rep. **43**, 185 (1999)].
8. P. Frick, S. L. Baliunas, D. Galyagin, et al., Astrophys. J. **483**, 426 (1997).
9. I. M. Livshits, in *Solntse v period smeny znaka polyarnostei magnitnogo polya (The Sun in a Period of Magnetic Field Reversal)* (GAO RAN, St. Petersburg, 2001), p. 241 [in Russian].
10. R. A. Gulyaev, Astron. Vestn. **40** (2006) (in press).
11. R. Howe, J. Christensen-Dalsgaard, F. Hill, et al., Science **287**, 2456 (2000).
12. E. Benevolenskaya and A. G. Kosovichev, Izv. Ross. Akad. Nauk, Ser. Fiz. (2006) (in press).

Translated by D. Gabuzda